



You have downloaded a document from
RE-BUŚ
repository of the University of Silesia in Katowice

Title: Ordering of [alpha]-FeCo phase in the nanocrystalline Fe_{83-x}CoxNb₃B₁₃Cu₁ (x = 6, 25 or 41.5) alloys

Author: Józef Zbroszczyk, Alina Młyńczyk, Jacek Olszewski, Wanda Ciurzyńska, Bolesław Wysłocki, Kamila Perduta, Józef Lelątko, Marcin Nabiałek

Citation style: Zbroszczyk Józef, Młyńczyk Alina, Olszewski Jacek, Ciurzyńska Wanda, Wysłocki Bolesław, Perduta Kamila, Lelątko Józef, Nabiałek Marcin. (2007) Ordering of [alpha]-FeCo phase in the nanocrystalline Fe_{83-x}CoxNb₃B₁₃Cu₁ (x = 6, 25 or 41.5) alloys. "Nukleonika" (Vol. 52, suppl. 1 (2007), s. 29-32).



Uznanie autorstwa - Użycie niekomercyjne - Bez utworów zależnych Polska - Licencja ta zezwala na rozpowszechnianie, przedstawianie i wykonywanie utworu jedynie w celach niekomercyjnych oraz pod warunkiem zachowania go w oryginalnej postaci (nie tworzenia utworów zależnych).



UNIwersYTET ŚLĄSKI
W KATOWICACH



Biblioteka
Uniwersytetu Śląskiego



Ministerstwo Nauki
i Szkolnictwa Wyższego

Ordering of α -FeCo phase in the nanocrystalline $\text{Fe}_{83-x}\text{Co}_x\text{Nb}_3\text{B}_{13}\text{Cu}_1$ ($x = 6, 25$ or 41.5) alloys

Józef Zbroszczyk,
Alina Młyńczyk,
Jacek Olszewski,
Wanda Ciurzyńska,
Bolesław Wysocki,
Kamila Perduta,
Józef Lelątko,
Marcin Nabiałek

Abstract. The microstructure and ordering of α -FeCo phase of the nanocrystalline $\text{Fe}_{83-x}\text{Co}_x\text{Nb}_3\text{B}_{13}\text{Cu}_1$ ($x = 6, 25$ or 41.5) alloys were investigated. We have stated that α -FeCo phase is atomically ordered in the $\text{Fe}_{83-x}\text{Co}_x\text{Nb}_3\text{B}_{13}\text{Cu}_1$ ($x = 25$ or 41.5) samples crystallized by the heat treatment in a furnace. However, after flash annealing (by current or laser) that phase is disordered. Moreover, we have found that Co concentration in the crystalline α -FeCo phase strongly depends on Co content in the as-quenched ribbons. The annealing conditions influence also the grain diameter of the crystalline phase. In the nanocrystalline alloys obtained by a flash annealing of the amorphous ribbons finer grains are present.

Key words: nanocrystalline alloys • microstructure • ordering • Mössbauer spectroscopy


Introduction

It is well known that conventional crystalline Fe-Co alloys in α -phase exhibit very large saturation magnetization [1]. The two phase FeCo-based nanocrystalline materials known as Hitperm [5, 8] are especially interesting because of their good magnetic properties at elevated temperatures. This results from high Curie temperatures of both, the crystalline α -FeCo phase and amorphous matrix [6]. The magnetic properties of those materials containing nanoscale-size magnetic grains, surrounded by an amorphous phase depend on their composition and microstructure [4]. The structure of those alloys is created during primary crystallization of amorphous precursors. It has been found [4, 6] that α -FeCo phase is atomically ordered in the nanocrystalline alloys obtained by heat treatment of rich in cobalt amorphous ribbons.

In this paper, we present results of studies which were undertaken in order to establish the effect of annealing conditions of amorphous ribbons on the atomic ordering of α -FeCo phase in the nanocrystalline $\text{Fe}_{83-x}\text{Co}_x\text{Nb}_3\text{B}_{13}\text{Cu}_1$ ($x = 6, 25$ or 41.5) alloys.

Experimental procedure

Ingots of the composition $\text{Fe}_{83-x}\text{Co}_x\text{Nb}_3\text{B}_{13}\text{Cu}_1$ ($x = 6, 25$ or 41.5) were prepared by induction melting in a protective argon atmosphere using high purity Fe, Co, Fe_3B , Nb and Cu components. Amorphous ribbons 10 mm wide and 22 μm thick were produced from those ingots by a single roller melt-spinning method.

J. Zbroszczyk, A. Młyńczyk, J. Olszewski,
W. Ciurzyńska, B. Wysocki, K. Perduta , M. Nabiałek
Institute of Physics,
Częstochowa University of Technology,
19 Armii Krajowej Str., 42-200 Częstochowa, Poland,
Tel./Fax: +48 34 3250795,
E-mail: kama@wip.pcz.pl

J. Lelątko
Institute of Materials Science,
University of Silesia,
12 Bankowa Str., 40-007 Katowice, Poland

Received: 20 June 2006
Accepted: 5 October 2006

Differential scanning calorimetry was used to find the crystallization temperature of the ribbons after rapid solidification. In these studies, the samples were annealed with the rate of 20 K/min up to 1000 K under an argon atmosphere. The nanocrystalline alloys were obtained by partial devitrification of the amorphous ribbons during the conventional or flash heat treatments. The conventional heat treatment was performed in a furnace at 650 K or 750 K for 10 min. The samples subjected to the flash heat treatment were annealed by DC current of $j = 5000 \text{ A/cm}^2$ density for 0.5 s or by YAG-Nd laser of pulse frequency equal to 180 Hz. The velocity of 2 mm diameter laser beam along the ribbon was equal to 1 mm/s. The amorphicity of the as-quenched alloys was testified by Mössbauer spectroscopy, X-ray diffraction and transmission electron microscopy. Due to the similarity of the atomic scattering factors of Fe and Co it is difficult to differentiate between the disordered and ordered α -FeCo phase by conventional X-ray diffraction, so the Mössbauer spectroscopy was used to determine atomic ordering of the crystalline phase in the nanocrystalline alloys. The transmission Mössbauer spectra were recorded at room temperature using a constant acceleration spectrometer with a $^{57}\text{Co}(\text{Rh})$ source of about 50 mCi activity and were analysed by Normos package [2]. Taking into account the parameters of the Mössbauer spectra corresponding to the crystalline phase (average magnetic hyperfine field and standard deviation of its distribution) and equations showing relations between these parameters and iron concentration and order parameters [3] the Bragg-Williams parameter and iron concentration in the crystalline phase were determined. Moreover, from Mössbauer spectra analysis the phase composition of the nanocrystalline samples was also found. The structure of the nanocrystalline samples were observed by a transmission electron microscope.

Results and discussion

The as-quenched alloys were fully amorphous which was confirmed by Mössbauer spectroscopy (Fig. 1). The Mössbauer spectra of those alloys consist of sextets with very broad and overlapped lines typical of an amorphous state. The hyperfine field distributions obtained from those spectra consist of at least two components which gives evidence of the presence of regions with different iron concentration.

The crystallization of these alloys takes place in two stages as is shown in DSC curves (Fig. 2). The first stage corresponds to the primary crystallization during which the partial transformation from the amorphous to nanoscale b.c.c. α -FeCo phase occurs. However, the second peak in DSC curves is related to the complete crystallization of the remaining intergranular phase. From the differential scanning calorimetry studies we have found that primary crystallization of the alloys investigated starts at about 660 K.

Figure 3 shows the transmission Mössbauer spectra obtained at room temperature for the partially crystallized $\text{Fe}_{83-x}\text{Co}_x\text{Nb}_3\text{B}_{13}\text{Cu}_1$ ($x = 6, 25$ or 41.5) alloys by the annealing of the amorphous ribbons at 650 or

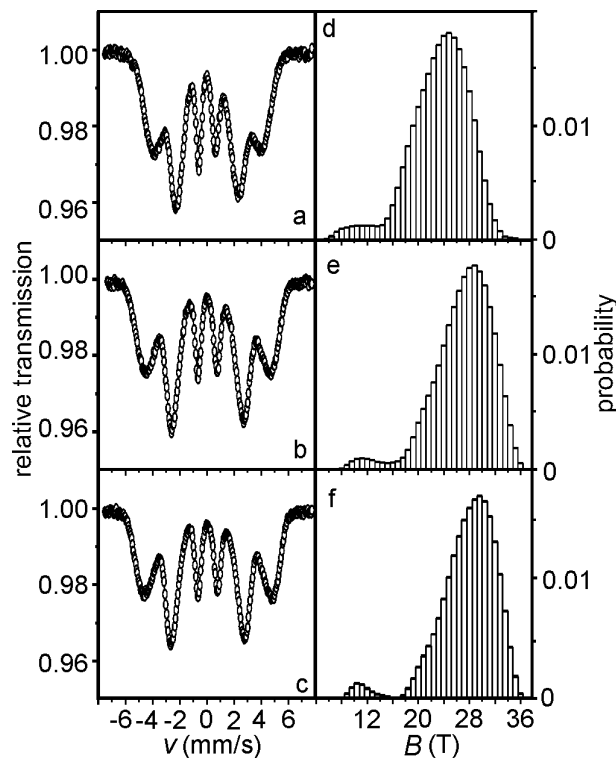


Fig. 1. Transmission Mössbauer spectra (a, b, c) and corresponding hyperfine field distributions (d, e, f) of the as-quenched $\text{Fe}_{83-x}\text{Co}_x\text{Nb}_3\text{B}_{13}\text{Cu}_1$ alloys: $x = 6$ (a, d), $x = 25$ (b, e), $x = 41.5$ (c, f).

750 K for 10 min. Mössbauer spectra of the samples annealed at 650 K for 10 min (Fig. 3a,b,c) consist of sextets with sharp lines related to α -FeCo grains and broad sextets corresponding to the remaining intergranular amorphous phase. The intensity of the sharp lines (Fig. 3d,e,f) increases after the annealing of the samples at 750 K for 10 min. Similar spectra were detected for the samples subjected to the flash annealing by the electric current or laser. These Mössbauer spectra were fitted with the combination of the Gaussian [3] and continuous magnetic hyperfine field distributions for the α -FeCo phase and intergranular amorphous phase, respectively.

The representative magnetic hyperfine field distributions obtained for the intergranular phase from the

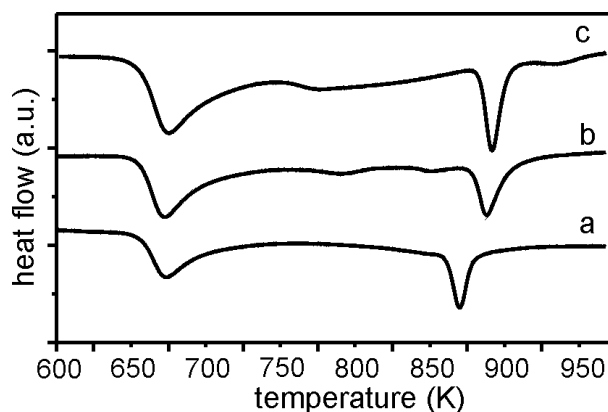


Fig. 2. Isochronal DSC curves for the as-quenched $\text{Fe}_{83-x}\text{Co}_x\text{Nb}_3\text{B}_{13}\text{Cu}_1$ alloys: $x = 6$ (a), $x = 25$ (b), $x = 41.5$ (c).

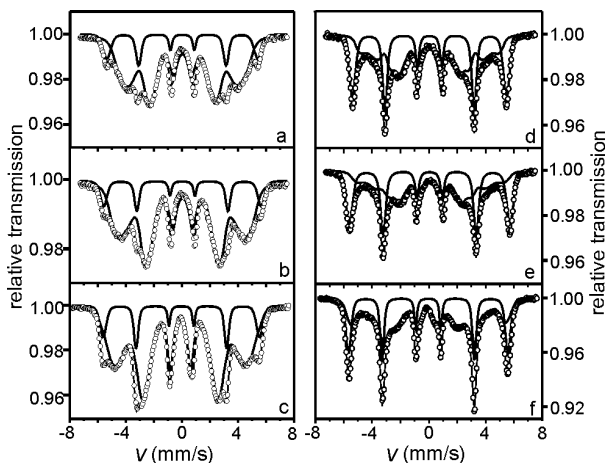


Fig. 3. Transmission Mössbauer spectra of the $\text{Fe}_{83-x}\text{Co}_x\text{Nb}_3\text{B}_{13}\text{Cu}_1$ alloys: annealed in the furnace at 650 K for 10 min (a, b, c) and 750 K for 10 min (d, e, f); $x = 6$ (a, d), $x = 25$ (b, e), $x = 41.5$ (c, f).

Mössbauer spectra of the nanocrystalline alloys are presented in Fig. 4. The magnetic hyperfine field distributions demonstrate the complex structure, and one can distinguish in them at least four components. The highest field component can be ascribed to the interface layer between α -FeCo grains and the amorphous matrix [7]. However, the other components in the magnetic hyperfine field distributions are related to the amorphous matrix. The obtained results indicate that the intergranular phase in the investigated nanocrystalline alloys obtained by the flash annealing is more homogeneous than in the samples heat treated in the furnace.

Data obtained from Mössbauer spectra analysis for the nanocrystalline alloys are collected in Table 1. The average magnetic hyperfine field at ^{57}Fe nuclei derived for as-quenched amorphous alloys is also included. It is seen that the value of the magnetic hyperfine field at ^{57}Fe nuclei for the as-quenched alloys depends on Co concentration which is in agreement with the Slater-Pauling theory [1]. Assuming that B and Nb atoms were

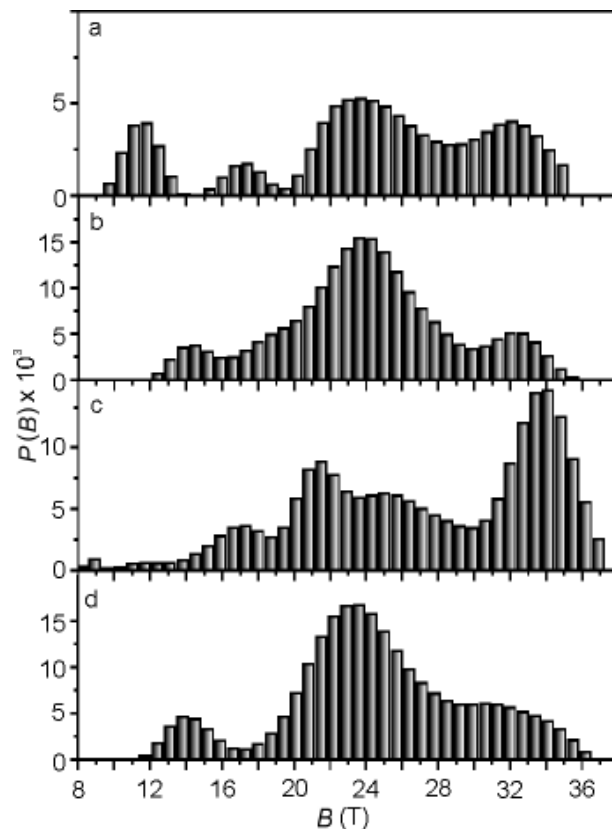


Fig. 4. Hyperfine field distributions of the intergranular phase for the $\text{Fe}_{83-x}\text{Co}_x\text{Nb}_3\text{B}_{13}\text{Cu}_1$ alloys: annealed in the furnace at 750 K for 10 min (a, c) and by current (b, d); $x = 25$ (a, b), $x = 41.5$ (c, d).

completely removed from the crystalline phase during the crystallization of the samples, the composition of that phase can be described as $\text{Fe}_{100-x}\text{Co}_x$.

From the results presented in Table 1, one can notice that Co concentration in the crystalline α -FeCo phase of the nanocrystalline alloys depends mainly on the chemical composition of the amorphous ribbons. Taking into account the values of the magnetic hyperfine field, standard deviation of the hyperfine field distributions

Table 1. Average hyperfine field (B_{am} and B_{cr}) of amorphous and crystalline phase, respectively, composition of the crystalline phase, relative contribution (V_{cr}) of the crystalline phase in the nanocrystalline sample and the Bragg-Williams order parameter (S) of the crystalline α -FeCo phase for the nanocrystalline $\text{Fe}_{83-x}\text{Co}_x\text{Nb}_3\text{B}_{13}\text{Cu}_1$ ($x = 6, 25$ or 41.5) alloys

Co content in samples	Annealing conditions	B_{am} (T)	B_{cr} (T)	Crystalline phase	V_{cr}	$S \pm 0.15S$
$x = 6$	as-quenched	23.30	–	–	–	–
	650 K/10 min	24.19	33.43	$\text{Fe}_{96}\text{Co}_4$	0.13	–
	750 K/10 min	23.18	33.47	$\text{Fe}_{96}\text{Co}_4$	0.37	–
$x = 25$	as-quenched	26.98	–	–	–	–
	650 K/10 min	26.66	34.96	$\text{Fe}_{59}\text{Co}_{41}$	0.14	0.8
	750 K/10 min	24.21	35.19	$\text{Fe}_{60}\text{Co}_{40}$	0.44	0.8
	Current annealing	24.04	36.14	$\text{Fe}_{67}\text{Co}_{33}$	0.41	–
	Laser annealing	25.70	35.88	$\text{Fe}_{62}\text{Co}_{38}$	0.23	–
$x = 41.5$	as-quenched	27.71	–	–	–	–
	650 K/10 min	27.26	34.65	$\text{Fe}_{50}\text{Co}_{50}$	0.16	0.5
	750 K/10 min	24.12	34.63	$\text{Fe}_{52}\text{Co}_{48}$	0.47	0.6
	Current annealing	24.39	35.13	$\text{Fe}_{53}\text{Co}_{47}$	0.32	–
	Laser annealing	24.75	34.71	$\text{Fe}_{48}\text{Co}_{52}$	0.30	–

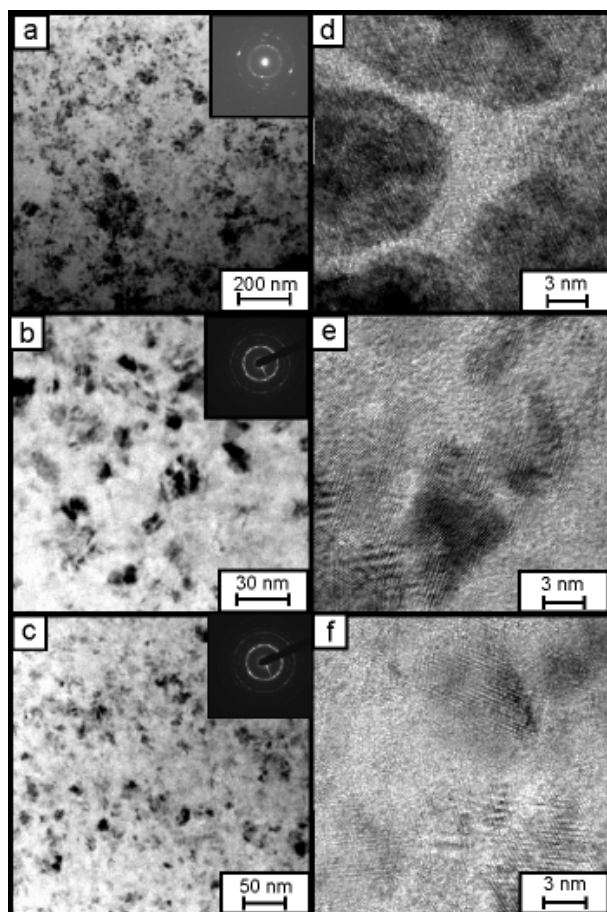


Fig. 5. Micrographs of the $\text{Fe}_{41.5}\text{Co}_{41.5}\text{Nb}_3\text{B}_{13}\text{Cu}_1$ alloys: annealed in the furnace at 750 K for 10 min (a, d), by current (b, e) and the laser (c, f); a, b, c – conventional resolution, d, e, f – high resolution.

and isomer shift corresponding to the crystalline α -FeCo phase, we have stated that it exhibits long-range atomic order [3] for the $\text{Fe}_{83-x}\text{Co}_x\text{Nb}_3\text{B}_{13}\text{Cu}_1$ ($x = 25$ or 41.5) alloys annealed in a furnace. The Bragg-Williams order parameter shows the highest value for the alloy containing 25 at.% of Co in the as-quenched state. However, α -FeCo phase in the nanocrystalline $\text{Fe}_{83-x}\text{Co}_x\text{Nb}_3\text{B}_{13}\text{Cu}_1$ ($x = 25$ or 41.5) alloys obtained by the flash annealing of the amorphous ribbons is completely disordered.

From transmission electron microscopy studies (Fig. 5), we have found that the annealing conditions influence also the crystalline grains diameter and their distribution in the amorphous matrix. In the nanocrystalline samples obtained by the conventional annealing of the amorphous ribbons, the crystalline grains with the diameter from 3 nm up to 50 nm are present (Fig. 5a). Furthermore, these grains are distributed irregularly and in some regions conglomerates of grains separated by the amorphous matrix are observed (Fig. 5b). However, the flash annealing allows

to obtain the nanocrystalline alloys with finer grain structure than in conventionally heat treated samples. The average diameter of α -FeCo grains is equal to 10 and 12.5 nm for the samples annealed by current and laser, respectively.

Conclusions

1. The ordering of α -FeCo phase in the nanocrystalline $\text{Fe}_{83-x}\text{Co}_x\text{Nb}_3\text{B}_{13}\text{Cu}_1$ ($x = 25$ or 41.5) alloys depends on annealing conditions. That phase is atomically ordered in the alloys obtained by annealing of the amorphous ribbons in the furnace. However, that phase is completely disordered in the alloys subjected to the flash annealing. Co content in the crystalline α -FeCo phase mainly depends on Co concentration in the amorphous samples.
2. The intergranular phase in the samples annealed by the flash annealing is more homogeneous than in the samples heat treated in the furnace.
3. The nanocrystalline alloys obtained by the flash annealing show finer grain structure.

Acknowledgments The paper was partially supported by the Ministry of Scientific Research and Information Technology (grant No. 4 T08A 02825).

References

1. Berkovitz A, Kneller E (1989) Magnetism and metallurgy. Academic Press, New York-London
2. Brand RA (1987) Improving the validity of hyperfine field distributions from magnetic alloys. Nucl Instrum Methods Phys Res B 28:398–416
3. Frąckowiak JE (1985) Determination of the long-range order parameter in the transition metal alloys using Mössbauer spectroscopy. Phys Status Solidi A 87;1:109–119
4. Hasiak M, Zbrozczyk J, Ciużyńska W *et al.* (2004) Crystallization and magnetic behaviour of $(\text{Fe}_{1-x}\text{Co}_x)_{85.4}\text{Zr}_{5.8}\text{Nb}_1\text{B}_{6.8}\text{Cu}_1$ ($x = 0, 0.1, 0.3, 0.5$) alloys. Phys Status Solidi C 1;12:3463–3467
5. Johnson F, Hughes P, Gallagher R *et al.* (2001) Structure and thermomagnetic properties of new FeCo-based nanocrystalline ferromagnets. IEEE Trans Mag 37;4:2261–2263
6. McHenry ME (1999) Amorphous and nanocrystalline materials for applications as soft magnets. Prog Mater Sci 44:291–433
7. Olszewski J, Zbrozczyk J, Fukunaga H *et al.* (2002) Transition from amorphous to nanocrystalline state in $\text{Fe}_{85.4}\text{Zr}_{6.8-x}\text{Nb}_x\text{B}_{6.8}\text{Cu}_1$ ($x = 0, 1$) alloys. J Magn Mater 241;2/3:381–389
8. Willard MA, Laughlin DE, McHenry ME *et al.* (1998) Structure and magnetic properties of $(\text{Fe}_{0.5}\text{Co}_{0.5})_{88}\text{Zr}_7\text{B}_4\text{Cu}_1$ nanocrystalline alloys. J Appl Phys 84;12:6773–6777